



## Gelatine microbubble as bioactive porogen in calcium phosphate cement

Kannaporn Pooput<sup>1,\*</sup>, Woranan Petcharoen<sup>2</sup>

<sup>1</sup>National Metal and Materials Technology Center (MTEC), 114 Phahonyothin Road, Khlong 1, Khlong Luang, Pathum Thani, Thailand

<sup>2</sup>Sirindhorn International Institute of Technology (SIIT), 99 Moo 18, Phahonyothin Road, Khlong 1, Khlong Luang, Pathum Thani, Thailand

Received 14 November 2018; Received in revised form 5 March 2019; Accepted 20 May 2019

### Abstract

*The objective of this study was to prepare instant macroporous calcium phosphate cement (CPC) with enhanced degradation rate and improved initial cell adhesion by simply incorporating lab-made gelatine microbubble (Gel MB) as dry porogen into the cement. From the study, it was found that viscosity of the cement paste was a key parameter to produce small or large macropores in the cements. Pore size was also determined by microbubble size, which was originally controlled by gelatine concentration in a bubble fabrication process. CPC with high porosity (60%) and acceptable cement setting time could be obtained from the study by incorporating 10 wt.% gelatine into the cement. Greater number of MC3T3-cells were found on the surface of the Gel MB loaded CPCs. The increase of initial cell adhesion may be attributed to protein molecules adhered on the cement surface and increase of surface roughness after porogen disintegration. In sum, a one-step composite cement paste production, proposed in the study, may be applicable for fabricating rapid macropores in CPCs with improved cell adhesion for bone tissue engineering applications.*

**Keywords:** calcium phosphate cement, gelatine, microbubble, macropores, cell adhesion

### I. Introduction

Hydroxyapatite-forming calcium phosphate cements (HAP-CPCs) have gained great interest for being used as bone graft substitutes since they are biocompatible, easy to mould and self-setting under physiological conditions without heat generation [1–4]. However, their degradation rate is very slow and initial cell adhesion on the cement surface is relatively poor, therefore limiting their use in tissue engineering applications. Numerous attempts have been made to produce macropores (larger than 50  $\mu\text{m}$ ) in HAP-CPCs by incorporation of additives, such as soluble porogens [5,6], gas-generating materials [7,8], surfactants [9] and degradable polymers [10,11] into the CPCs or even using 3D printing [12]. However, there are some limitations using these additives to fabricate HAP-CPCs with macroporous structure. For example, several of these approaches can only be applied for pre-set cements. Adding large portion

of additives can potentially cause toxicity. In addition, some porogens can only produce macropores within weeks or months, limiting new tissue replacement.

Recently, a new method was proposed by mixing cement paste with biocompatible foaming agent prepared from albumen [13] or gelatine [14] to produce instant macroporous cements with enhanced degradation of the HAP-CPCs. Foams are produced by rapid stirring of solution containing these naturally derived materials with a mixer. The foamed solution is then immediately transferred and mixed with cement paste. Even though this approach has been proved able to manufacture macroporous cements, it is still difficult to handle. Handling mixer and heating apparatus, required for preparing gelatine solution, might not be convenient for clinical use. To improve handling of foaming preparation, we proposed to fabricate gelatine foam in dry form first and subsequently mix it with the CPC to prepare instant macroporous scaffold.

Microbubbles (MBs) are composed of a gaseous core surrounded with lipid, protein or polymer shell. They

\*Corresponding author: tel: +66 2 5646500 ext.4450, e-mail: [kannaporn.poo@mtec.or.th](mailto:kannaporn.poo@mtec.or.th)

are commonly used as ultrasound-enhanced agents for molecular imaging and drug delivery applications [15–17]. MBs as contrast agents are on microscale, ranging from 1 to 10  $\mu\text{m}$  in diameter [18]. To the best of our knowledge, there is no report on using dry MB as porogen to create macropores in HAP-CPCs.

One of the required properties for materials to be used as scaffold in tissue engineering applications is good initial cell adhesion. Several methods have been reported to improve cell adhesion property of the HAP-CPCs by incorporation of protein sequence such as RGD, known as integrin-recognition site to promote cell attachment [19], or fibronectin, which is a general biomolecule that can anchor cells to proteoglycan and collagen into the CPC [20]. Even though these techniques can promote cell attachment, high cost including difficulty in handling still limits their use. Gelatine is derived from collagen, which is a protein found in animal bone or skin. It is biocompatible and completely degradable in physiological environment [21]. Several studies report that gelatine can also improve cell adhesion [22,23].

The aims of this study were to develop a simple preparation of instant macroporous cement for use in clinics by preparing gelatine microbubbles as dry porogen and to validate its efficiency to increase degradation rate and to improve cell adhesion of the cement. Physical, chemical, mechanical and biological properties of the cements were explored. The influence of powder to liquid ratio ( $P/L$ ) on pore formation and porosity was also evaluated.

## II. Experimental procedure

### 2.1. Preparation of cement powder

Tetracalcium phosphate (TTCP,  $\text{Ca}_4(\text{PO}_4)_2\text{O}$ ) powder was synthesized by a solid-state reaction at 1450 °C of a mixture of 0.95 mol of calcium carbonate ( $\text{CaCO}_3$ , Carlo Erba Reagenti, Italy) and 1.0 mol of dicalcium phosphate anhydrous (DCPA,  $\text{CaHPO}_4$ , Sigma Aldrich, Singapore), followed by dry quenching at room temperature. The synthesized TTCP was dry-milled in a planetary ball mill and the powder with median particle size of about  $12 \pm 0.5 \mu\text{m}$  was chosen for the study. The commercial DCPA powder was also milled in ethanol before use. An average size of DCPA powder of  $2 \pm 0.5 \mu\text{m}$  was used for compounding the cement. CPC powder was prepared by mixing an equivalent molar mass of TTCP and DCPA powders.

### 2.2. Fabrication of Gel MB embedded cement

Fabrication started with preparation of gelatine microbubble (Gel MB) from gelatine solutions having different concentrations (5, 10 and 20 wt./vol.% gelatine). 10 ml of gelatine solution, which was prepared by dissolving gelatine powder (Himedia, India) in distilled water at 45 °C, was homogenized with a disperser (IKA Inc, IKA T25 Dispersers) for 3 min under ambient conditions and speed of 5000 rpm. The prepared gelatine

bubbles were quickly quenched in liquid nitrogen before lyophilizing for 24 h at 0.03 mbar vacuum in a freeze dryer (Thermo Super Modulyo Freeze Dryer). The obtained dry Gel MB was cut into rectangular pieces of dimensions approximately 1.5 mm  $\times$  1.5 mm with sharp blade and kept in a desiccator before use. Bubble formation and microbubble size were studied by optical microscope (Olympus, IX71) connected with a digital camera (Olympus, DP72). A small piece of Gel MB was immersed in sodium phosphate buffer, which was used as liquid part for cement formulation in this study. Gel MB size was determined directly from images captured by optical microscope (five pieces of each dry Gel MB were used for the measurement).

Gel MB embedded cements were prepared by mixing various amounts of Gel MB (5 and 10 wt.% Gel MB) with CPC powder before liquid part was added. The obtained CPC pastes were then introduced in Teflon mould and allowed to set at room temperature before further characterization. The gas foaming can occur in cement when the cement paste has sufficiently low viscosity. In the study, two different powder to liquid ratios were chosen:  $P/L = 2.50$  and  $2.25$ . Other  $P/L$  ratios were previously examined, but only these two ratios gave sufficiently low viscosity and good mechanical strength (compressive strength of CPC prepared at interested  $P/L$  without any additive was higher than 30 MPa after 1 day incubation in phosphate buffer saline).

### 2.3. Characterization

Initial and final setting times were measured using a Gillmore needle. The initial and final setting times are defined as when a light needle (113.4 g in mass, and 2.13 mm in diameter) and a heavy needle (453.6 g in mass, and 1.06 mm in diameter) fail to make perceptible indentation on the sample surface. Each measurement was performed three times and the average value was calculated and presented.

The compressive strength of the incubated CPC samples was measured by using a universal testing machine (Instron Model 55R4502) with a crosshead speed of 1 mm/min ( $n = 5$ ). The sample specimens were prepared by mixing cement powders and liquid under desired  $P/L$  ratios. The obtained mixture was poured into a stainless steel mould (4 mm diameter  $\times$  8 mm height) and kept at room temperature for 1 h before removing from mould and immersing in phosphate buffer saline (PBS) at 37 °C for 7 days.

The embedded Gel MB CPC pastes were poured into 1 cm  $\times$  1 cm  $\times$  1 cm Teflon mould and allowed to harden at room temperature for 1 h. The cement was further incubated in PBS at 37 °C for 7 days. Afterwards, the cement samples were removed from their moulds and immersed in acetone to stop setting reactions. Dry samples were ground by hand and characterized by powder X-ray diffractometer (PANalytical, X'Pert PRO) using copper  $K\alpha$  radiation generated at 40 kV and 30 mA. Scans were performed between  $20^\circ < 2\theta < 60^\circ$  at

1 °/min, step size 0.01° and step time 0.6 s. In addition, the specimens were coated with gold before investigating HA formation by scanning electron microscopy (SEM, Hitachi, high vacuum FE-SEM SU8030). The size of hydroxyapatite crystal was measured directly from SEM micrographs (five areas were chosen and length and width of individual crystals were measured and averaged).

Porosity was determined from the samples incubated in PBS at 37 °C for 7 days, subsequently kept in an oven at 200 °C for 24 h and finally cooled to room temperature. Each dried sample was weighed ( $W_0$ ) and then placed in a known-weight ( $W_1$ ) specific gravity bottle filled with DI water. The evacuation under vacuum was performed for 10 min to remove air in the sample. The total weight of the specimen and the bottle was recorded as  $W_2$ . The sample was subsequently removed from the bottle, rapidly blotted and weighed ( $W_3$ ). The porosity ( $P$ ) of the sample was calculated using the following equation:

$$P = \frac{W_3 - W_0}{W_3 + W_1 - W_2} \times 100 \quad (1)$$

Gelatine leaching from CPC samples was studied by monitoring dissolution of Gel MB in incubated solution. The bicinchoninic acid protein assay (BCA assay; Pierce Biotechnologies, USA) was used to investigate gelatine leaching behaviour. The principle of the BCA assay relies on the formation of a  $\text{Cu}^{2+}$  protein complex under alkaline conditions, followed by reduction of the  $\text{Cu}^{2+}$  to  $\text{Cu}^{1+}$  by protein in alkaline medium that has been developed to a purple-blue-coloured solution [24]. Each cement sample was incubated in 1.5 ml of PBS at 37 °C for 3–24 h, and 1–7 days. The incubated PBS solution was collected and tested with BCA working reagents. Light absorption of the resulting solutions was measured at 595 nm and compared with the values obtained from solutions of defined gelatine concentrations (0.01–5 mg/ml). Incubated PBS solutions of cements without Gel MB were used as blanks. All experiments were performed in triplicate.

The CPC samples were also characterized by Fourier transform infrared spectroscopy (FTIR; Perkin Elmer System 2000) to detect the presence of gelatine in the CPC composites. The CPC samples were manually crushed with pestle and mortar into fine powder before testing with FTIR (4000–400  $\text{cm}^{-1}$ , 1.5 mg of sample in 100 mg of KBr).

#### 2.4. Cell proliferation study

MC3T3-E1 cells (ATCC, CRL-2593) were maintained using established cell culture protocols. Cells were cultivated in flasks (150  $\text{cm}^2$  surface area) at 37 °C with a humidified atmosphere at 5%  $\text{CO}_2$  in DMEM cell culture medium, supplemented with 10 vol.% of bovine fetal serum and 1 vol.% penicillin, changing the media every 2 days. At 90% confluence, cells were harvested by rinsing with 2.5 g/l trypsin solution and incubated at 37 °C until cells detached. Cells were washed again

with PBS. Then, cells were re-suspended in DMEM and ready for further study.

MC3T3-E1 cells were seeded directly onto the CPC samples with and without Gel MB at a density of  $1 \times 10^4$  cells/ $\text{cm}^2$ . Cells were allowed to attach to the sample for 1, 3 and 7 days in the culture medium at 37 °C and 5%  $\text{CO}_2$ . Culture medium was changed every 2 days. After the defined period of time, the cells were tested with Alamar Blue assay. Fluorescence emission intensity at 590 nm with excitation at 560 nm, which is proportional to the number of cells adhered on the samples, was collected.

Cell morphology and attachment on the cement samples with and without gelatine addition was observed by SEM and fluorescence microscopy. For the SEM, after 1 day of culture, the deposited cells were fixed with 4 wt./vol.% paraformaldehyde for 4 h at 4 °C and rinsed with PBS (pH 7.4) and subsequently dehydrated by passing the sample through a series of graded ethanol concentrations (30, 50, 70, 90 and 100 vol.% ethanol) for about 15 min each. The samples were then placed in a second 100% ethanol solution to ensure that water was completely removed. The dehydrated samples were further dried in a critical-point dryer (Baltec, CPD 030) before gold sputtering for cell morphology examination by SEM (Hitachi, S3400N). For fluorescence imaging, samples with cultured cells were rinsed twice with PBS and fixed with 4 wt./vol.% paraformaldehyde for 30 min at room temperature. After three time washing with PBS, the samples were incubated with 0.5 vol.% Triton-X 100 in PBS for 5 min. Then, actin filaments were stained by incubating the samples with rhodamine phalloidin (Invitrogen, Eugene, OR, USA) whereas cell nucleus was stained with 4',6-diamidino-2-phenylindole (DAPI, Sigma-Aldrich, USA). The samples were observed under a fluorescence microscope (Olympus, IX71).

### III. Results and discussion

#### 3.1. Characterization of Gel MB

Size and morphology of the dry gelatine microbubbles (Gel MB), fabricated from different gelatine solutions are shown in Fig. 1. The prepared Gel MB showed a core-shell structure. During homogenization under ambient environment, air was incorporated into the solution, resulting in bubble formation in gelatine solution. After quick freezing in liquid nitrogen and lyophilization, air bubbles were kept stable in gelatine envelope. Since in the study gelatine was not cross-linked, it was easily gelled and ready to be dissolved in water. When the Gel MBs contacted water, bubbles were immediately formed.

The average microbubble size for 5, 10 and 20 wt./vol.% gelatine was approximately 25, 40 and 100  $\mu\text{m}$  in diameter, respectively (Fig. 1a). Bubble formation significantly depends on the magnitude of liquid viscosity [25]. Bubbles could slowly grow to the larger

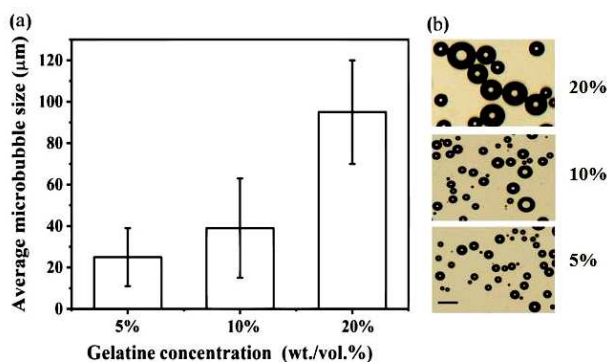


**Figure 1.** Gel MB average size prepared from gelatine solutions having different concentrations (5, 10 and 20 wt./vol.%) (a) and optical images of gelatine microbubbles dispersed in sodium phosphate buffer (bar = 100 μm) (b)

size by viscous resistance. In the study, 20 wt./vol.% gelatine solution was the highest viscosity that could create large microbubbles. We also explored bubble formation prepared from higher viscosity gelatine solutions (25 and 30 wt./vol.% gelatine) and found that large bubbles were difficult to form. The majority of bubbles was smaller than 50 μm (the results are not shown here). Because 20 wt./vol.% gelatine solution could produce the largest microbubbles, we used this concentration for preparing Gel MB to fabricate composite cements.

### 3.2. Cement setting time

Setting times of the cements containing different concentrations of the Gel MB prepared at two different  $P/L$

ratios are shown in Table 1. The cements prepared by using less amount of liquid ( $P/L = 2.50$ ) set faster than those prepared with greater liquid content ( $P/L = 2.25$ ). This behaviour is normally found when the less amount of liquid is used in the cement recipe [4,5]. For the cements containing Gel MB, it was found that increasing gelatine amount in CPC composites could slightly reduce initial setting time. Gelatine may increase cement cohesiveness, resulting in greater resistance to light-weight needle penetration. Several studies have reported that gelling agent, such as gelatine, can improve cement cohesion [7,14]. However, the cement composites containing gelatine showed delayed final setting time compared with those without gelatine. This negative effect on final setting time may be attributed to the viscosity increment of CPC paste after adding Gel MB. Ion diffusion in the paste therefore is lowered, resulting in longer final setting time. This effect was more prominent when greater amount of Gel MB was added to the CPC for both CPCs prepared at  $P/L = 2.50$  and 2.25 (Table 1).

### 3.3. Crystal structure and phase characterization

Figure 2 shows XRD patterns of composite cements containing different Gel MB contents prepared at  $P/L = 2.50$  and 2.25 after incubation in PBS for 7 days. The marked peaks in the figures correspond to characteristic peaks of hydroxyapatite (HAP), according to JCPDS crystallographic database (JCPDS 00-009-0432). It is clear that HAP peaks were found in all CPC samples. Also, all six CPC samples exhibited similar XRD intensity. SEM was used to characterize morphology of

**Table 1.** Initial and final setting times, compressive strength and porosity of CPCs

Cement	Initial setting time [min]	Final setting time [min]	Compressive strength [MPa]	Porosity [%]
$P/L = 2.50$				
0 wt.% Gel MB	10 ± 1	25 ± 1	37.3 ± 2.2	9.0 ± 1.4
5 wt.% Gel MB	10 ± 1	28 ± 1	28.5 ± 2.3	12.5 ± 1.9
10 wt.% Gel MB	7 ± 1	35 ± 2	19.2 ± 3.6	24.0 ± 2.8
$P/L = 2.25$				
0 wt.% Gel MB	13 ± 1	27 ± 1	33.1 ± 1.4	14.5 ± 2.3
5 wt.% Gel MB	12 ± 1	32 ± 1	13.8 ± 3.5	29.5 ± 1.1
10 wt.% Gel MB	10 ± 1	43 ± 1	5.5 ± 2.1	59.0 ± 2.9

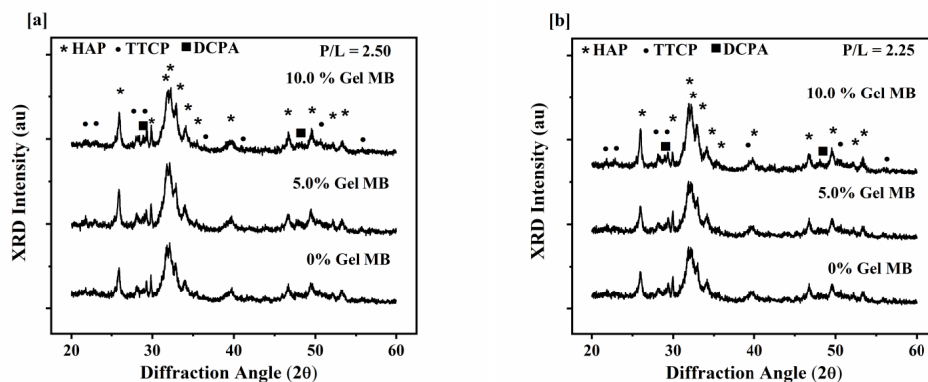


**Figure 2.** XRD patterns of CPCs containing different Gel MB contents prepared at: a)  $P/L = 2.50$  and b)  $P/L = 2.25$ , after immersion in PBS for 7 days

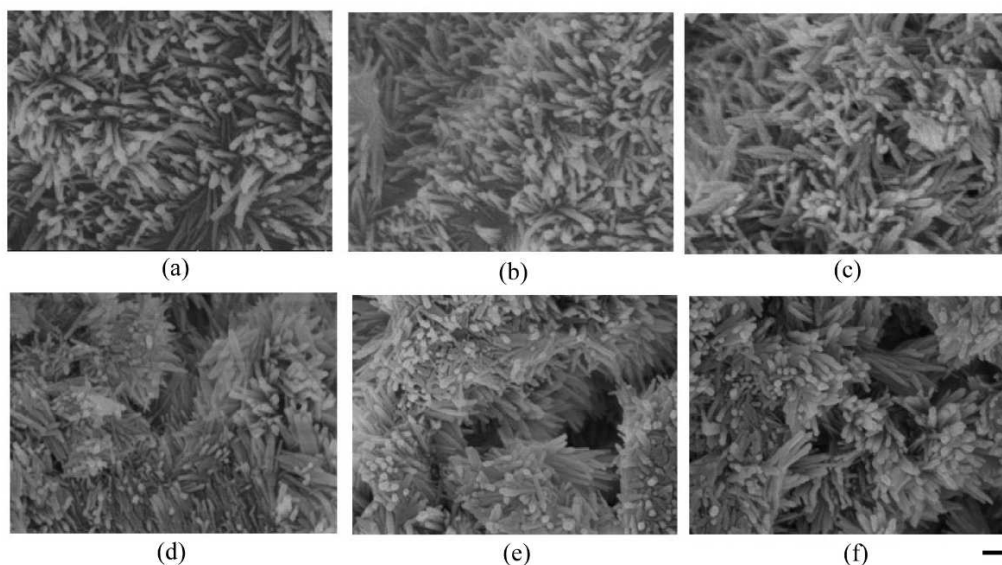


**Figure 3.** SEM micrographs of cements prepared at  $P/L = 2.50$  containing: a) 0, b) 5 and c) 10 wt.% Gel MB and at  $P/L = 2.25$  containing: d) 0, e) 5 and f) 10 wt.% Gel MB, after immersion in PBS for 7 days (bar = 200 nm)

**Table 2.** Average size of the rod-like hydroxyapatite crystals measured by SEM

Cement	Width [nm]	Length [nm]
$P/L = 2.50$		
0 wt.% Gel MB	$40 \pm 4$	$260 \pm 20$
5 wt.% Gel MB	$41 \pm 4$	$262 \pm 22$
10 wt.% Gel MB	$41 \pm 5$	$260 \pm 23$
$P/L = 2.25$		
0 wt.% Gel MB	$39 \pm 5$	$260 \pm 22$
5 wt.% Gel MB	$41 \pm 4$	$263 \pm 18$
10 wt.% Gel MB	$40 \pm 5$	$265 \pm 17$

the cement (Fig. 3). The CPCs containing different Gel MB concentrations (0, 5 and 10 wt.%), prepared at two  $P/L$  ratios, had similar microstructure. The nanosized rod-like crystals of HAP entangled among the particles were observed in all CPC samples. Average size of the HAP crystals was shown in Table 2. It is clearly seen that HAP crystal size was comparable for all samples.

### 3.4. Compressive strength and porosity

Compressive strength (CS) and porosity of the cements are shown in Table 1. CS of the CPC composites having  $P/L = 2.50$  varied approximately between 19 and 37 MPa whereas CS was roughly between 5 and 33 MPa for the composites having  $P/L = 2.25$ . It is apparent that CS of both types of the CPC composites decreased with increasing Gel MB content. In contrast, porosity of cements increased with increasing Gel MB content. The effect of porogen content on both CS and porosity was more prominent in CPCs prepared at  $P/L = 2.25$ . This result indicated that  $P/L$  ratio was an important factor determining pore formation in the CPC. CPCs prepared at  $P/L = 2.50$  had greater viscosity. It was difficult for bubbles to form and stay stable in the CPC paste until the cement completely hardened. Even with adding greater amount of Gel MB in the CPC paste ( $P/L = 2.50$ ), porosity in the cement did not sharply increase, as opposed to what it was found

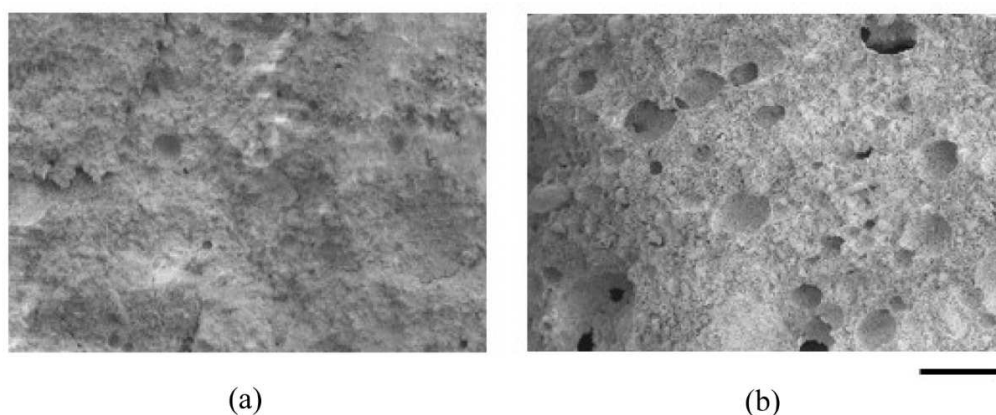


**Figure 4.** SEM micrographs of cements after 7 days of PBS incubation: a) cements prepared at  $P/L = 2.50$  with 5 wt.% Gel MB and b) those prepared at  $P/L = 2.25$  with 5 wt.% Gel MB (scale bar = 100  $\mu\text{m}$ )

in composite cements prepared at  $P/L = 2.25$ . CPCs ( $P/L = 2.50$ ) containing 10 wt.% Gel MB and that comprising of 5 wt.% Gel MB had approximately 24% and 12% porosity, respectively. In contrast, CPCs with lower viscosity ( $P/L = 2.25$ ) containing 10 wt.% Gel MB and that composed of 5 wt.% Gel MB had approximately 60% and 30% porosity, respectively. CPC paste viscosity does not only affect porosity but also pore size. In the study, it is found that the CPCs containing Gel MB prepared at  $P/L = 2.25$  primarily contained larger pores compared to the CPCs prepared at  $P/L = 2.50$  as clearly seen in Fig. 4. The CPCs without Gel MB were dense and contained only macropores smaller than  $50\ \mu\text{m}$ . Macropores larger than  $50\ \mu\text{m}$  in CPC can be obtained when appropriate  $P/L$  ratio is chosen. These findings are also confirmed by other studies [7–9,26].

Generally, HAP-CPCs without adding porogen comprise of only macropores smaller than  $50\ \mu\text{m}$ . To be used as scaffold, CPCs must have macroporous structure with pore diameter larger than  $50\ \mu\text{m}$ . The role of these macropores is to guide and support tissue ingrowth within the material so that angiogenesis can take place along with the progressive bioresorption of the scaffold [27].

### 3.5. Gelatine leaching

Leaching behaviours of uncross-linked gelatine were studied using BCA assay and are shown in Fig. 5. Cumulative detected amount of protein (gelatine) in PBS at  $37\ ^\circ\text{C}$  at different times was monitored. It is obvious that Gel MBs easily degraded in PBS solution. Gel MB could be completely leached out (100% detected protein concentration) after 3 and 4 days incubation in PBS for the CPCs prepared at  $P/L = 2.25$  and those at  $P/L = 2.50$ , respectively. Gel MB degraded more than 50% within 6 h incubation for both types of the CPCs. Results from FTIR confirmed what was found in BCA assay study as shown in Fig. 6. Gelatine has amide II band corresponding to the band at approximately  $1530\ \text{cm}^{-1}$ . After incubating the CPC containing

10 wt.% Gel MB prepared at  $P/L = 2.25$  and that fabricated at  $P/L = 2.50$  in PBS for 3 and 4 days, respectively, the specimens were manually crushed into powder and tested with the FTIR. It is apparent that there was no amide II band in both types of CPCs, indicating there was no gelatine remained in the tested CPC specimens.

The finding from gelatine leaching study was in agreement with what was found in porosity measurement. CPCs prepared at  $P/L = 2.25$  contained larger pores with higher porosity than those prepared at  $P/L = 2.50$ . PBS solution could flow more easily into the cement specimens prepared at  $P/L = 2.25$ , resulting in faster gelatine leaching.

Gelatine leaching rate may also play a key role in HAP conversion. The HAP-based CPC used in this study was a mixture of an equivalent molar mass of TTCP and DCPA. Non-stoichiometric hydroxyapatite ( $\text{Ca}_{10-x}(\text{PO}_4)_{6-x}(\text{OH})_{2+x}$ ) is a reaction product. Some studies have shown that adding porogens into the CPC can both prolong final setting time and interrupt HAP phase conversion [5,7]. Hence, slow setting and decrease in HAP peak intensity in XRD are observed. In our study it is found that an incorporation of the Gel MB delayed the final setting of the cements but XRD intensity of HAP peaks for all CPC samples was comparable after incubation in PBS for 7 days. The reason behind this may come from the fast gelatine degradation in PBS. Gelatine used in the study was not cross-linked. Therefore, it was easy to disintegrate it in water. We explored HAP phase conversion after 24 h PBS incubation and found that XRD intensity of HAP peaks of the CPCs containing Gel MB was a bit lower than those without Gel MB (the results are not included here). However, with continued PBS incubation, gelatine was leaching more. In parallel, HAP formation kept continuing. After gelatine was completely removed (3 and 4 days for CPCs prepared at  $P/L = 2.25$  and  $2.50$ , respectively), HAP conversion occurred freely, resulting in similar

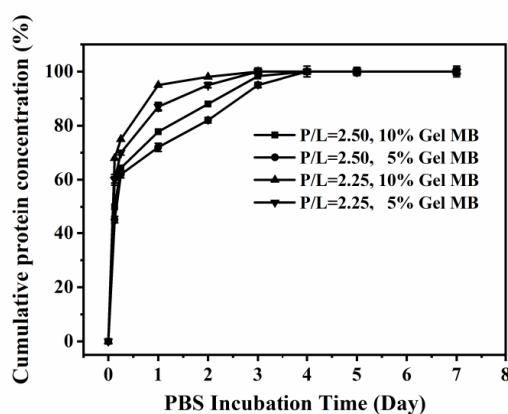


Figure 5. Cumulative detected gelatine concentration as a function of PBS incubation time using BCA assay, for CPC composites prepared at  $P/L = 2.50$  and  $2.25$ , containing 5 and 10 wt.% Gel MB

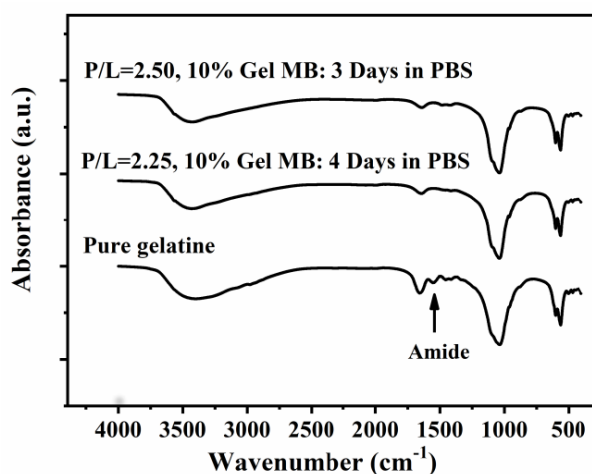


Figure 6. Comparison of FTIR spectra of pure gelatine and CPCs containing 10 wt.% Gel MB prepared at  $P/L = 2.50$  and  $2.25$  after soaking in PBS

XRD intensity of HAP peaks for all CPC samples. This is also why we found all CPC specimens showed similar microstructure exhibiting rod-like HAP crystals in scanning electron micrographs as shown in Fig. 3.

### 3.6. *In vitro* studies

Proliferation of pre-osteoblast cells (MC3T3-E1) using Alamar Blue assay of CPCs containing different Gel MB contents after incubating cells for different periods of time was evaluated as shown in Fig. 7. It is found that the CPC without any additive had limited number of ad-

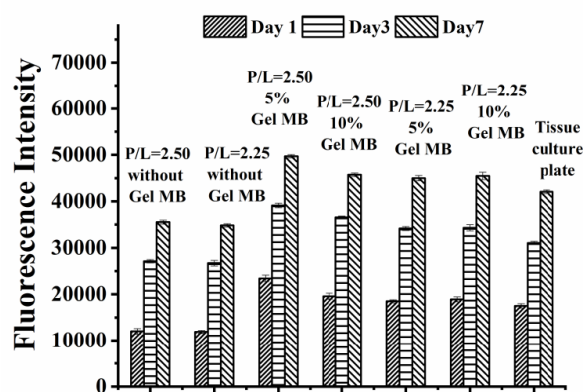


Figure 7. Cell proliferation on CPCs embedded with various concentrations of Gel MB by Alamar Blue assay

hering cells compared to those containing Gel MB and tissue culture plate. However, adhering cells exhibited cytoplasmic expansion indicating that they were healthy (Fig. 8a). This finding tells us that the pristine CPC was non-toxic but its initial cell adhesion was poor. On the contrary, greater number of healthy cells were found attached on the CPCs containing Gel MB as evidenced in Fig. 8b. The results of the cytoskeleton and nuclear staining from fluorescent image as shown in Fig. 8c confirmed that numerous MC3T3-E1 cells cultured on the CPC containing Gel MB exhibited well spread with a good cytoskeleton. Also, the numbers of cells on Gel MB embedded CPCs prepared by both  $P/L = 2.50$  and  $2.25$  were higher than those on tissue culture plate. The results indicated that incorporation of Gel MB into the CPC could enhance cell adhesion. Even though gelatine was rapidly leached out from the cement sample, some binding protein still existed on the surface of the sample. As a result, greater number of cells were found on the surface of CPCs containing Gel MB compared to those on CPCs without gelatine. Several studies have incorporated gelatine into scaffolds to improve biocompatibility, cell adhesion and cell differentiation for bone tissue engineering [29–31]. Gelatine as bioactive additive is normally chemically modified or crosslinked with scaffolds for prolonged effect. Therefore, the enhancement of the interaction of cells and material surface was more prominent than what we found in this study.

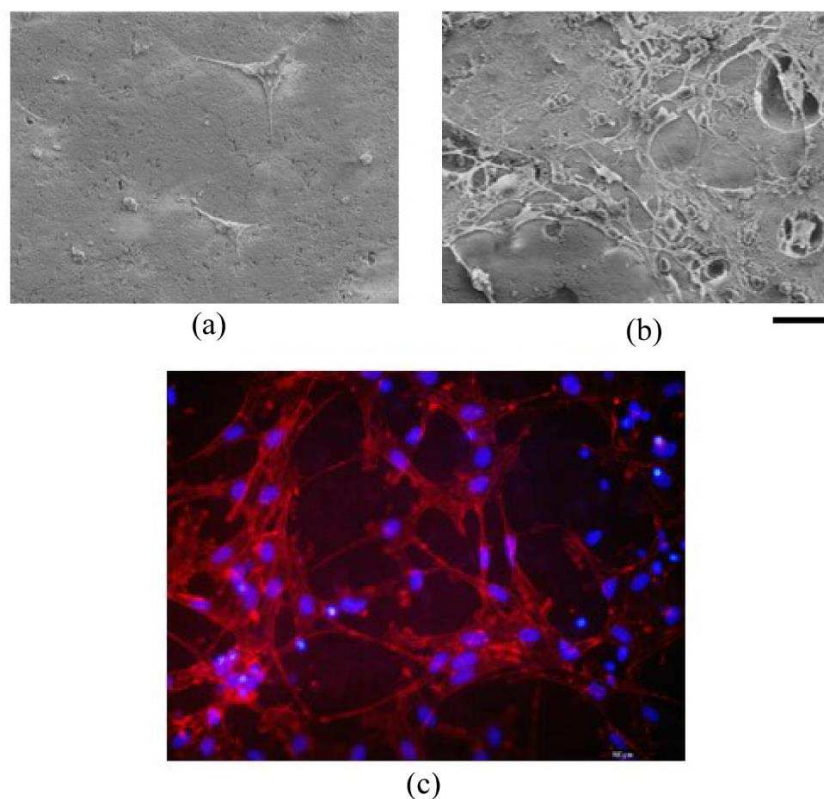


Figure 8. SEM micrographs of cellular adhesion on the surface of CPCs prepared at  $P/L = 2.25$  containing (a) 0 wt.% Gel MB and (b) 5 wt.% Gel MB after culturing MC3T3-E1 cells for 24 h (Scale bar = 50  $\mu\text{m}$ ). Nuclei (blue) and actin (red) were stained with DAPI and phalloidin, respectively. A representative fluorescence image (c) of MC3T3-E1 stained with nuclei and actin on the surface of CPCs prepared at  $P/L = 2.25$  containing 5 wt.% Gel MB after cell culture for 24 h

It is interesting that MC3T3-E1 cells were more prone to adhere to CPCs containing Gel MB prepared by  $P/L = 2.50$  than those prepared by  $P/L = 2.25$ . Difference in surface topography might be a reason for this finding [28]. Surface of CPCs prepared at different  $P/L$  ratios is shown in Fig. 4. It is clearly seen that CPCs prepared by  $P/L = 2.50$  had smaller pore size than those prepared by  $P/L = 2.25$ . The smaller pores may be easier for cells to anchor and subsequently proliferate. Tissue engineering integrates material engineering and cell biology together. Scaffold for bone tissue should have pore size larger than  $50\ \mu\text{m}$  with good initial cell adhesion. These two characteristics should go parallel. From our study, it is indicated that pore size and cell adhesion property should be considered in a design and fabrication of scaffold. CPCs with macroporous structure and improved cell attachment could be achieved by incorporating porogen containing protein binding molecules such as gelatine in the system.

#### IV. Conclusions

Macroporous CPCs could be successfully prepared by simply mixing dry gelatine microbubble with the CPC recipe. From the study, it has been shown that cement paste viscosity was a key parameter to produce macropores or micropores in the CPC. Prolonged final setting time was observed with gelatine addition. Hydroxyapatite phase conversion reached equilibrium after gelatine completely leached out of the cement. Strength of the cement was inversely proportional to porosity. Macroporous CPCs prepared from gelatine microbubble were cell friendly and were able to promote cell adhesion. Using soluble dry foam to produce macropores may potentially be an alternative method for preparing macroporous scaffold for bone tissue engineering applications.

**Acknowledgement:** The authors gratefully acknowledge the financial support received from the National Metal and Materials Technology Center (MTEC) of the Ministry of Science and Technology, Thailand. Also, the authors appreciate an assistance for BCA assay study from Dr. Katanchalee Mai-Ngam's lab group: Satrawut Charoenla, Warobon Noppakunmongkolchai and Dr. Jitlada Sansatsadeekul

#### References

1. A.J. Ambard, L. Mueninghoff, "Calcium phosphate cement: Review of mechanical and biological properties", *J. Prosthodont.*, **15** (2016) 321–328.
2. J. Zhang, W. Liu, V. Schnitzler, F. Tancret, J.M. Bouler, "Calcium phosphate cements for bone substitution: Chemistry, handling and mechanical properties", *Acta Biomater.*, **10** (2014) 1035–1049.
3. K. Hurtle, J. Neubauer, M. Bohner, N. Doebelin, F. Goetz-Neunhoeffler, "Effect of amorphous phases during the hydraulic conversion of alpha-TCP into calcium-deficient hydroxyapatite", *Acta Biomater.*, **10** (2014) 3931–3941.
4. E.F. Burguera, F. Guitian, L.C. Chow, "A water setting tetracalcium phosphate-dicalcium phosphate dehydrate cement", *J. Biomed. Mater. Res. A*, **71** (2004) 275–282.
5. H. Xu, E. Burguera, L. Carey, "Strong, macroporous, and in situ-setting calcium phosphate cement-layered structures", *Biomaterials*, **28** (2007) 3786–3796.
6. F. He, Y. Yang, J. Ye, "Tailoring the pore structure and property of porous biphasic calcium phosphate ceramics by NaCl additive", *Ceram. Int.*, **42** (2016) 14679–14684.
7. A. Almiral, G. Larrecq, J.A. Delgado, S. Martinez, J.A. Planell, M.P. Ginebra, "Fabrication of low temperature macroporous hydroxyapatite scaffold by foaming and hydrolysis of and  $\alpha$ -TCP paste", *Biomaterials*, **25** (2004) 3671–3680.
8. S. Hesaraki, D. Sharifi, "Investigation of an effervescent additive as porogenic agent for bone cement macroporosity", *Biomed. Mater. Eng.*, **17** (2007) 29–38.
9. S. Sarda, M. Nilsson, M. Balcells, E. Fernandez, "Influence of surfactant molecules as air-entraining agent for bone cement macroporosity", *J. Biomed. Mater. Res. A*, **65** (2003) 215–221.
10. R.P. Lanao, S.C.G. Leeuwenburgh, J.G.C. Wolke, J.A. Jansen, "In vitro degradation rate of apatitic calcium phosphate cement with incorporated PLGA microspheres", *Acta Biomater.*, **7** (2011) 3459–3468.
11. A. Roy, S. Jhunjhunwala, E. Bayer, M. Fedorchak, S.R. Little, P.N. Kumta, "Porous calcium phosphate-poly (lactic-co-glycolic) acid composite bone cement: A viable tunable drug delivery system", *Mater. Sci. Eng. C*, **59** (2016) 92–101.
12. A.R. Akkineni, Y. Luo, M. Schumacher, B. Nies, A. Lode, M. Gelinsky, "3D plotting of growth factor loaded calcium phosphate cement scaffold", *Acta Biomater.*, **27** (2015) 264–274.
13. M. Genebra, J. Delgado, I. Harr, A. Almirall, S. Del Valle, J.A. Planell, "Factors affecting the structure and properties of an injectable self-setting calcium phosphate foam", *J. Biomed. Mater. Res. A*, **80** (2007) 351–361.
14. E. Montufar, T. Traykova, E. Schacht, L. Ambrosio, M. Santin, J. Planell, M. Genebra, "Self-hardening calcium deficient hydroxyapatite/gelatin foams for bone regeneration", *J. Mater. Sci. Mater. Med.*, **21** (2010) 863–869.
15. S.R. Sirsi, M.A. Borden, "Advances in ultrasound mediated gene therapy using microbubble contrast agents", *Theranostics*, **2** (2012) 1208–1222.
16. S. Qin, C.F. Caskey, K.W. Ferrara, "Ultrasound contrast microbubbles in imaging and therapy: physical principles and engineering", *Phys. Med. Biol.*, **4** (2009) R27–R57.
17. I. Lentacker, S.C. De Smedt, N.N. Sanders, "Drug loaded microbubble design for ultrasound triggered delivery", *Soft Matter*, **5** (2009) 2161–2170.
18. S. Sirsi, M. Borden, "State-of-the-art materials for ultrasound-triggered drug delivery", *Adv. Drug Deliv. Rev.*, **72** (2014) 3–14.
19. M.C. Echave, P. Sanchez, J.L. Pedraz, G. Orive, "Progress of gelatin-based 3D approaches for bone regeneration", *J. Drug Deliv. Sci. Technol.*, **42** (2017) 63–74.
20. S.L. Bellis, "Advantages of RGD peptides for directing cell association with biomaterials", *Biomaterials*, **32** (2011) 4205–4210.
21. J. van den Dolder, G.N. Bancroft, V.I. Sikavitsas, P.H. Spauwen, A.G. Mikos, J.A. Jansen, "Effect of fibronectin and collagen I-coated titanium fiber mesh on prolifera-



- tion and differentiation of osteogenic cells”, *Tissue Eng.*, **9** (2003) 505–515.
22. L. Bakhtiari, H.R. Rezaie, S.M. Hosseinalipour, M.A. Shokrgozar, “Investigation of biphasic calcium phosphate/gelatin nanocomposite scaffolds as a bone tissue engineering”, *Ceram. Int.*, **36** (2010) 2421–2426.
  23. A.J. Kuijpers, G.H. Engbers, J. Krijgsveld, S.A. Zaat, J. Dankert, J. Feijen, “Cross-linking and characterization of gelatin matrices for biomedical applications”, *J. Biomater. Sci. Polym. Ed.*, **11** (2000) 225–243.
  24. P.K. Smith, R.L. Krohn, G.T. Hermanson, A.K. Mallia, F.H. Gartner, M.D. Provenzano, E.K. Fujimoto, N.M. Goeke, B.J. Olson, D.C. Klenk, “Measurement of protein using bicinchoninic acid”, *Anal. Biochem.*, **150** (1985) 72–85.
  25. K. Pancholi, E. Stride, M. Edirisinghe, “Dynamics of bubble formation in highly viscous liquids”, *Langmuir*, **24** (2008) 4388–4393.
  26. J. Unosson, E.B. Montufar, H. Engqvist, M.P. Ginebra, C. Persson, “Brushite foams – the effect of Tween 80 and Pluronic F-127 on foam porosity and mechanical properties”, *J. Biomed. Mater. Res. B*, **104B** (2016) 67–77.
  27. M. Bohner, “Design of ceramic-based cements and putties for bone graft substitution”, *Eur. Cells Mater.*, **20** (2010) 1–12.
  28. D.O. Costa, P.D. Prowse, T. Chrones, S.M. Sims, D.W. Hamilton, A.S. Rizkalla, S.J. Dixon, “The differential regulation of osteoblast and osteoclast activity by surface topography of hydroxyapatite coatings”, *Biomaterials*, **34** (2013) 7215–7226.
  29. D. Li, H. Sun, L. Jiang, K. Zhang, W. Liu, Y. Zhu, J. Fangteng, C. Shi, L. Zhao, H. Sun, B. Yang, “Enhanced biocompatibility of PLGA nanofibers with gelatin/nanohydroxyapatite bone biomimetics incorporation”, *ACS Appl. Mater. Interfaces*, **6** (2014) 9402–9410.
  30. C.K. Chiu, J. Ferreira, T.J.M. Luo, H. Geng, F.C. Lin, C.C. Ko, “Direct scaffolding of biomimetic hydroxyapatite-gelatin nanocomposites”, *J. Mater. Sci. Mater. Med.*, **9** (2012) 2115–2126.
  31. C.K. Chiu, D.J. Lee, H. Chen, L.C. Chow, C.C. Ko, “In-situ hybridization of calcium silicate and hydroxyapatite-gelatin nanocomposites enhances physical property and in vitro osteogenesis”, *J. Mater. Sci. Mater. Med.*, **2** (2015) 1–14.